J. Gen. Appl. Microbiol., **69**, 301–308 (2023)
doi 10.2323/jgam.2023.08.004

jGAM

Full Paper

Gallic acid fermentation by metabolically engineered *Escherichia coli* producing *p*-hydroxybenzoate hydroxylase from *Hylemonella gracilis* NS1

(Received July 12, 2023; Accepted August 16, 2023; J-STAGE Advance publication date: August 30, 2023)

Nozomi Katsuki,[1] Shunsuke Masuo,[1] Noriyuki Nukui,[1] Hajime Minakawa,[1] and Naoki Takaya[1,*]

[1] *Faculty of Life and Environmental Sciences, Microbiology Research Center for Sustainability, University of Tsukuba, 1-1-1 Tennodai, Tsukuba, Ibaraki 305-8572, Japan*

Plant-derived phenolic gallic acid (GA) is an important raw material for antioxidants and food additives. Efforts to ferment GA using microbial processes have aimed at minimizing production costs and environmental load using enzymes that hydroxylate *p*-hydroxybenzoate and protocatechuate (PCA). Here, we found a *p*-hydroxybenzoate hydroxylase (PobA) in the bacterium *Hylemonella gracilis* NS1 (HgPobA) with 1.5-fold more hydroxylation activity than that from *Pseudomonas aeruginosa* PAO1 and thus converted PCA to GA more efficiently. The PCA hydroxylation activity of HgPobA was improved by introducing the amino acid substitutions L207V/Y393F or T302A/Y393F. These mutants had 2.9- and 3.7-fold lower K_m^{app} for PCA than wild-type HgPobA. An *Escherichia coli* strain that reinforces shikimate pathway metabolism and produces HgPobA when cultured for 60 h generated 0.27 g L^{-1} of GA. This is the first report of fermenting glucose to generate GA using a natural enzyme from the PobA family. The *E. coli* strain harboring the HgPobA L207V/Y393F mutant increased GA production to 0.56 g L^{-1}. During the early stages of culture, GA was fermented at a 10-fold higher rate by a strain producing either HgPobA L207V/Y393F or T302A/Y393F compared with wild-type HgPobA, which agreed with the high k_{cat}^{app}/K_m^{app} PCA values of this mutant. We enhanced a PobA isozyme and its PCA hydroxylating function to efficiently and cost-effectively ferment GA.

Keywords: *Escherichia coli*; monooxygenase; *p*-hydroxybenzoate hydroxylase; protocatechuate; shikimate pathway

Introduction

The phenolic compound 3,4,5-trihydroxybenzoic acid (gallic acid; GA) is derived from gallnuts, sumac, hazel, tea leaves, and oak bark (Haslam and Cai, 1994). Due to its polyhydric phenol structure, GA has antioxidant and antibacterial properties, and it is a raw material for food additives, antiseptics, cosmetics, and pharmaceuticals (Badhani et al., 2015; Diaz-Gomez et al., 2013). Propyl gallate and other gallate esters also serve as food additives (Aruoma et al., 1983), and GA derivatives are found in adhesives, coatings, and electronic components (Kinugawa et al., 2016; Sileika et al., 2013). Pyrogallol is a decarboxylated product of GA used as a dye and in the organic synthesis of valuable compounds (Kim et al., 2011). Gallic acid is currently hydrolyzed from plant-derived tannins during a process where acids and bases are catalysts, which burdens environmental loads. Therefore alternative catalysts have been developed such as anionic resins and enzymes (Lara-Victoriano, 2017; Luo et al., 2018; Rommel and Wrolstad, 1993).

The fermentation of GA using genetically engineered bacteria is a potential alternative method for producing GA (Chen et al., 2017; Chen et al., 2022; Kambourakis et al., 2000), which is a useful material for bio-based pyrogallol (Huo et al., 2018; Wang et al., 2018). One strategy for microbial GA production applies genetically manipulated *Escherichia coli* that produces chorismate pyruvate lyase (4-hydroxybenzoate synthase) to convert the endogenous shikimate pathway intermediate, chorismate, to ferment glucose and produce *para*-hydroxybenzoate (*p*HBA) (Chen et al., 2017). Another strategy also mediates the shikimate pathway to heterogeneously produce 3-dehydroshikimate dehydratase that converts the pathway intermediate 3-dehydroshikimate (DHS) to protocatechuic

*Corresponding author: Naoki Takaya, Faculty of Life and Environmental Sciences, University of Tsukuba, Tsukuba, Ibaraki 305-8572, Japan.
Tel: 81-29-853-4937 E-mail: takaya.naoki.ge@u.tsukuba.ac.jp

None of the authors of this manuscript has any financial or personal relationship with other people or organizations that could inappropriately influence their work.

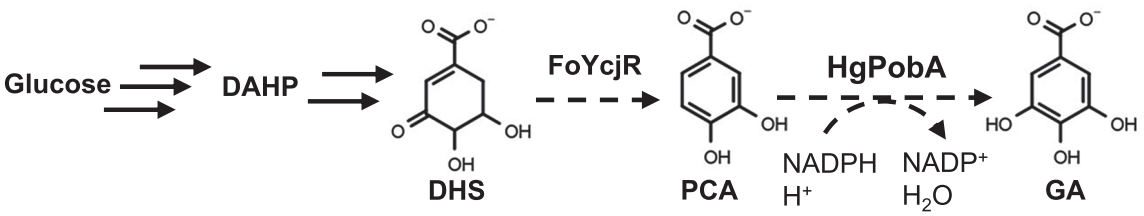

Fig. 1. Gallic acid fermentation strategy.

Solid and dashed arrows indicate endogenous and heterogeneous reactions, respectively. DAHP, 3-deoxy-D-arabinoheptulosonate 7-phosphate; DHS, 3-dehydroshikimic acid. FoYcjR, *ycjR* encoding DHS dehydratase from *Fusarium oxysporum* f. sp. Lycopersici; HgPobA, *pobA* encoding *p*-hydroxybenzoate hydroxylase from *Hylemonella gracilis* NS1.

Table 1. Primer sequences (5′ → 3′) .

Primer	Sequence
HgF	ATCACCACAGCCAGGATCCGAATTCAAGCTACCCCACCCGTAC
HgR	TTAAGCATTATGCGGCCGCAAGCTTCAGGCGCCGAAATCCAAG
PaF	ATCACCACAGCCAGGATCCGAATTCAAAGACTCAAGTCGCCATC
PaR	TTAAGCATTATGCGGCCGCAAGCTTCTCGATTTCCTCGTAGGG
Y393F (F)	GTGGCCGAGAACTTCGTCGGCCTGCCC
(R)	GGGCAGGCCGACGAAGTTCTCGGCCAC
L207V (F)	GTGCACCACGAGGTGATCTACGTGAAC
(R)	GTTCACGTAGATCACCTCGTGGTGCAC
T302A (F)	CATCGTGCCGCCCGCGGGGGCCAAGGGCC
(R)	GGCCCTTGGCCCCCGCGGGCGGCACGATG

F, forward; R, reverse.

acid (PCA) (Fig. 1) (Chen et al., 2022; Kambourakis et al., 2000). The final step in both of these strategies is facilitated by *p*HBA hydroxylases (E.C. 1.14.13.2) produced in the same strains to convert *p*HBA or PCA to GA.

Efficient production of GA requires amino acid substitutions in *p*HBA hydroxylases (PobA); these enable high turnover of PCA hydroxylation to generate GA, because native PobA preferentially hydroxylates *p*HBA over PCA as a substrate (Spector and Massey, 1972). The active site mutant Y385F of *Pseudomonas aeruginosa* PobA (PaPobA) hydroxylates PCA more rapidly than native PaPobA (Entsch et al., 1991). This mutant ferments GA in metabolically engineered *E. coli* using glucose as the raw material (Kambourakis et al., 2000). The authors found T294A/Y385F and L199V/Y385F mutations that increased the PCA hydroxylation rate 16- and 29-fold more than native PaPobA (Chen et al., 2017; Moriwaki et al., 2019). Recent random mutagenesis studies have discovered PaPobA mutants with more hydroxylation activity against PCA (Chen et al., 2022; Maxel et al., 2020). More effort has been directed towards PaPobA and its mutants for microbial GA fermentation, than to exploring novel enzymes that could efficiently catalyze PCA hydroxylation.

This study mined genomic databases and found a novel PobA from *Hylemonella gracilis* NS1 (HgPobA) that had 1.5-fold higher hydroxylation activity against PCA than PaPobA. We constructed *H. gracilis* L207V/Y393F and T302A/Y393F mutants with 3- and 2-fold lower K_m ^{app} values for PCA. We also designed a biosynthetic pathway to produce 3-dehydroshikimate dehydratase and HgPobA or its derivatives in *E. coli* (Fig. 1) that fermented up to 0.56 ± 0.01 g L^{-1} GA.

Material and methods

Strains and media. We prepared plasmids, produced recombinant proteins, and fermented GA (Wako Pure Chemical Industries, Osaka, Japan) in *E. coli* using NEB turbo (New England Biolabs, Ipswich, MA, USA), BL21 Star (DE3) (Invitrogen, Carlsbad, CA, USA), and NST37 (DE3) (Masuo et al., 2016), respectively. Cells were cultured in Luria Bertani (LB) medium (10 g tryptone, 5 g yeast extract, and 10 g NaCl/ L^{-1}) and GA was fermented in medium containing 10 g tryptone, 5 g yeast extract, 24 g Na_2HPO_4, 12 g KH_2PO_4, 0.5 g NaCl, 1 g NH_4Cl, 0.5 g $MgSO_4$ $7H_2O$, 15 mg $CaCl_2$, 50 mg thiamine-HCl, 2 mL/ L^{-1} of Hutner's trace element solution (Hutner, 1950), and 1% glucose (Fujita et al., 2013). The plasmids were maintained in media containing 30 mg L^{-1} kanamycin sulfate and 40 mg L^{-1} ampicillin sodium.

Plasmid construction. A DNA fragment of the *hgpobA* gene (NCBI accession number, WP_131280663) was chemically synthesized, and amplified by PCR using the primers HgF and HgR (Table 1). The amplified fragment was cloned into pRSFduet-1 that had been digested with *Eco*RI and *Hin*dIII using NEBuilder HiFi DNA Assembly Master Mix (New England Biolabs) to yield pRSF-*hgpobA*. A fragment encoding *papobA* was amplified from the total DNA of *P. aeruginosa* JCM 14847 (RIKEN Bioresource Center, Wako, Japan) using the primers PaF and PaR (Table 1), and cloned into pRSFduet-1 to generate pRSF-*papobA*. Thereafter, mutant pRSF-*hgpobA* was amplified by PCR using \ circularized pRSF-*hgpobA* as a template and the primers Y393F_F and Y393F_R, L207V_F and L207V_R, and T302A_F and T302A_R for mutagenesis of Y393F, L207V, and T302A, respectively (Table 1).

The resulting DNA fragments were digested with *Dpn*I and transformed into *E. coli* NEB turbo to yield pRSF-*hgpobA* L207V/Y393F and *hgpobA* T302A/Y393F.

Preparation of recombinant HgPobA. *Escherichia coli* BL21 Star (DE3) cells harboring pRSF-*hgpobA* and its derivatives were cultured overnight in 5 mL of LB medium containing 30 mg L^{-1} kanamycin sulfate at 37°C. Portions (1 mL) were inoculated into 100 mL of the same medium, and stirred at 120 rpm at 37°C until the optical density (OD) at 600 nm reached 0.6. Thereafter, 0.4 mM isopropyl *β*-D-1-thiogalactopyranoside (IPTG) was added to the medium, and the culture was stirred at 120 rpm at 20°C for 12 h. The cells were sedimented by centrifugation, suspended in 20 mM Tris-HCl, pH 7.9 (buffer A), and disrupted by ultrasonication. Cell debris was removed from the sonicate by centrifugation at 10,000 × *g* for 15 min, then proteins were purified using a HisTrap FF column (Cytiva, Marlborough, MA, USA) equilibrated with buffer A containing 20 mM imidazole. Bound proteins were washed with 10 column volumes of buffer A containing 20 mM imidazole, then eluted from the column with buffer A containing 300 mM imidazole. Eluents were concentrated, suspended in buffer A, then passed through Amicon Ultra-0.5 mL filters with a 10 kDa cutoff (Merck, Darmstadt, Germany). Protein concentrations in the filtrate were determined by the Bradford method using Protein Assay Dye Reagent (Bio-Rad Laboratories, Hercules, CA, USA) as described by the manufacturer.

High-performance liquid chromatography. We analyzed *p*HBA, PCA, and GA and cofactors by high-performance liquid chromatography (HPLC) using an Agilent 1260 Infinity system (Agilent Technologies, Santa Clara, CA, USA), a Purospher Star RP-18 endcapped column with a particle size of 5 *μ*m (Millipore-Merck, Billerica, MA, USA). The mobile phase comprised 20 mM phosphoric acid pH 2.5 (solvent A) and methanol (solvent B) at a flow rate of 1.0 mL min^{-1} and the column temperature was 30°C.

Purified HgPobA was boiled for 3 min, and the supernatant was analyzed with a mobile phase comprising a 60:40 ratio of solvent A: solvent B) to determine cofactors. The column temperature was 30°C, and absorption was monitored at 450 nm.

Reactions (100 *μ*L) containing 20 mM Tris-HCl (pH 7.9), 5 mM NADPH, 10 *μ*M FAD, 1 mM *p*HBA or PCA, and 10 *μ*g purified PobA were incubated at 30°C for 5 min, terminated by adding 100 *μ*L of 2 M HCl, and analyzed by HPLC to determine *p*HBA, PCA, and GA. The column temperature was 30°C and the mobile phase comprised 90:10 solvent A: solvent B. Absorption at 210 nm was quantified.

Steady-state kinetics. Reactions (100 *μ*L) were started by adding 0–1 mM *p*HBA (Wako Pure Chemical Industries, Osaka, Japan) or PCA (Oriental Yeast Tokyo, Japan) to 20 mM Tris-HCl (pH 7.9) containing 10 *μ*M FAD, 0.25 mM NAD(P)H, and purified PobAs. Absorbance at 340 nm was monitored at 25°C using a U3900 spectrophotometer (Hitachi). We quantified NAD(P)H (Oriental Yeast) using a molar absorption coefficient of 6300 M^{-1} cm^{-1}. The initial velocity of NAD(P)H consumption was determined in triplicate, and fitted to a Michaelis-Menten equation to calculate apparent Michaelis (K_m^{app}) and kinetic (k_{cat}^{app}) constants.

Fermentation of GA. Bacterial strains were constructed as follows. The cDNA of the *ycjR* gene from *Fusarium oxysporum* f. sp. Lycopersici (UniProt accession no: A0A0D2XXI8) was synthesized and cloned into pRSFduet-1 to generate pRSF-*foycjR*. Plasmid RSF-*hgpobA* and its derivatives were digested with *Eco*RI and *Hind*III, and their inserted sequences were cloned into pETduet-1 that was previously digested with the same restriction enzymes to generate pET-*hgpobA*, *hgpobA* L207V/Y393F, and *hgpobA* T302A/Y393F. The plasmids were transformed into *E. coli* NST37 (DE3) harboring pRSF-*foycjR* and rotary shaken at 180 rpm overnight in 5 mL of LB medium at 37°C to generate *E. coli* G1, G2, and G3 strains. Thereafter, cultures (1 mL) were inoculated into 100 mL of fermentation medium containing 1% glucose in 500-mL conical flasks. When the OD reached 0.6, 1 mM IPTG was added and the cells were further incubated at 28°C and shaken at 120 rpm for 60 h. Glucose (2 mL; 500 g L^{-1}) was added every 24 h. Glucose concentrations were quantified using glucose CII test kits (Fujifilm Wako Pure Chemical Corporation, Osaka, Japan). The signal intensity of gels was quantified using ImageJ software (Schneider et al., 2012).

Results

Identification and characterization of HgPobA

We predicted PobA proteins with 60%–70% amino acid sequence similarity to PaPobA using BlastP and the NCBI database. We identified a PobA-like protein from *H. gracilis* NS1 (HgPobA) with 63% similarity. Recombinant HgPobA was prepared, and SDS-PAGE confirmed its calculated purity and molecular mass (Fig. 2A). The protein spectrum showed absorption peaks at 375 and 450 nm (Fig. 2B). The HPLC findings showed that HgPobA contained FAD and negligible amounts of FMN (Fig. 2C), indicating that HgPobA uses FAD as a prosthetic group. Since the FAD content was 0.52 mol/mol protein, we measured the enzyme activity against an excess of FAD (10 *μ*M). Specific activities for *p*HBA- and PCA-dependent NADPH oxidation were 6.9 ± 0.1 and 1.5 ± 0.1 *μ*mol min^{-1} mg^{-1}, respectively (Table 2). Those for 2,4-dihydroxybenzoate and 4-aminobenzoate were 1.0 ± 0.2 and 0.061 ± 0.003 *μ*mol min^{-1} mg^{-1}, respectively (Table 2). The HgPobA activity for PCA was 3.5-fold higher than that of PaPobA, and replacing NADPH with NADH resulted in activity of < 0.01 *μ*mol min^{-1} mg^{-1}.

We analyzed PCA and GA production by HgPobA in 5-min reactions containing an excess of NADPH (5 mM). The reaction generated 760 and 25 *μ*M of PCA and GA respectively (Fig. 3A–C), with 1 mM *p*HBA as the substrate, and 140 *μ*M GA with 1 mM PCA as the substrate. Reactions of PaPobA under the same conditions generated 820 *μ*M of PCA and 6.1 *μ*M of GA, but only 40 *μ*M of GA when PCA was the substrate, which was less than that generated by HgPobA (Fig. 3D). These results indicated that HgPobA, unlike PaPobA, is a novel hydroxylase for *p*HBA and PCA that prefers PCA.

Fitting the *p*HBA and PCA-dependent NADPH oxidation

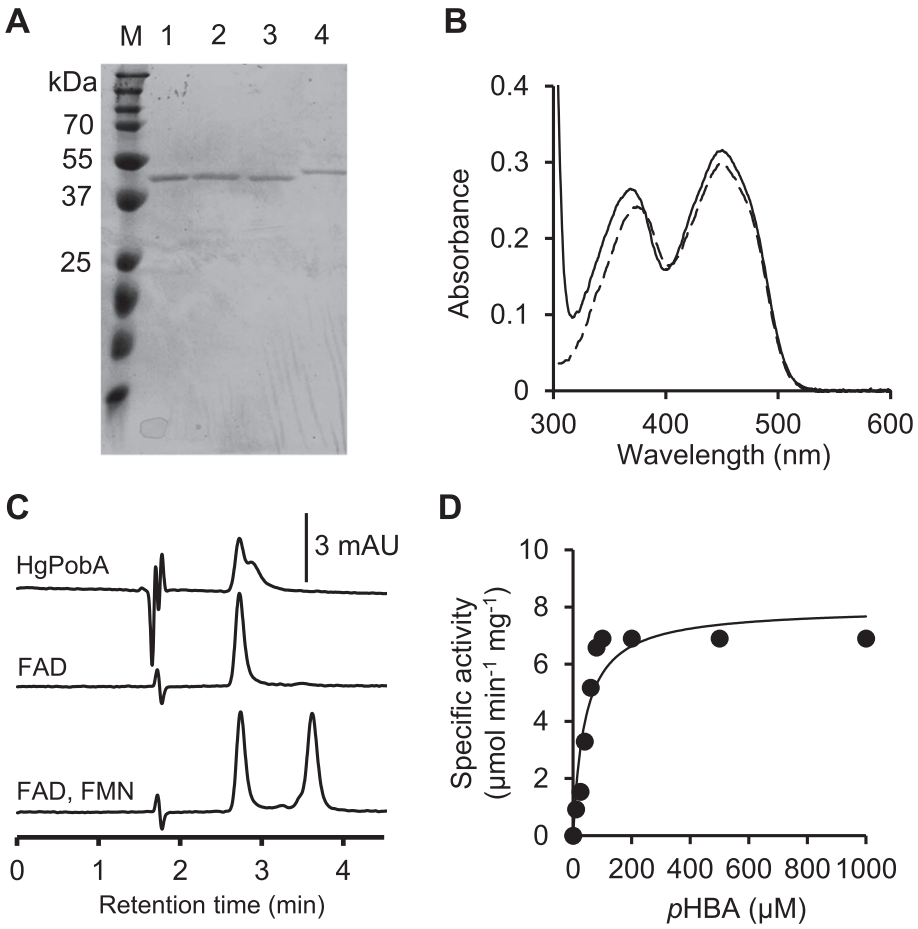

Fig. 2. Biochemical characterizations of HgPobA.

A. Proteins resolved by SDS-PAGE. M, molecular weight marker; 1, recombinant HgPobA; 2, recombinant HgPobA L207V/Y393F; 3, recombinant HgPobA T302A/Y393F; 4, recombinant PaPobA (1 μg each). B. Absorption spectra of HgPobA (54 μM) (solid line), and FAD (26 μM) (dashed line) in 20 mM Tris-HCl (pH 7.9). C. Analysis of cofactors in HgPobA. Purified HgPobA was boiled, centrifuged, and supernatants analyzed by HPLC are shown as absorption at 210 nm. D. Specific activities of HgPobA for various concentrations of *p*HBA and 0.25 mM NADPH in 20 mM Tris-HCl (pH 7.9). Data were fitted to the Michaelis-Menten equation.

Table 2. Specific activity of HgPobA and PaPobA for various aromatic compounds.

Enzyme	Specific activity (μmol min^{-1} mg^{-1})				
	*p*HBA	PCA	2-Hydroxy-benzoate	2,4-Dihydroxy-benzoate	4-Amino-benzoate
HgPobA	6.9 ± 0.1	1.5 ± 0.1	< 0.01	1.0 ± 0.2	0.061 ± 0.003
PaPobA	7.0 ± 0.5	0.43 ± 0.07	< 0.01	0.34 ± 0.08	0.021 ± 0.004

Initial velocity of NADPH consumption was measured in 20 mM Tris-HCl (pH 7.9) containing 0.25 mM NADPH, 10 μM FAD, 1 mM aromatic substrate, and purified PobA protein at 25°C. Data are shown as means ± standard deviation (n = 3).

rates to the Michaelis-Menten equation indicated that the apparent Michaelis (K_m^{app}) and rate (k_{cat}^{app})-constants for the reaction using *p*HBA were 35 ± 14 μM and 5.6 ± 0.6 s^{-1}, compared with those of PaPobA (24 ± 7 μM and 4.7 ± 0.3 s^{-1}; Fig. 2D, Table 3). The apparent K_m^{app} and k_{cat}^{app} for PCA were 260 ± 30 μM and 0.74 ± 0.03 s^{-1}, respectively, and the apparent k_{cat}^{app} was 1.5-fold higher than that of PaPobA (0.51 ± 0.02 s^{-1}, Table 3). These findings indicated that the higher turnover of HgPobA could partly explain the relatively greater PCA hydroxylation activity compared with that of PaPobA.

Efficient coupling of HgPobA and PCA

The PaPobA reactions often uncouple NADPH oxidation and the hydroxylation of non-preferred substrates such as PCA to spontaneously reduce O_2 to hydrogen peroxide (Eshchrich et al., 1993; Moriwaki et al., 2019). Our findings were consistent with these in that the HgPobA reaction was not stoichiometric and generated less PCA and GA than oxidized NADPH (Fig. 3A). We compared NADPH oxidation with PCA and GA production to determine the stoichiometry of the reaction. After the complete consumption of 0.5 mM NADPH, we quantified the amount of

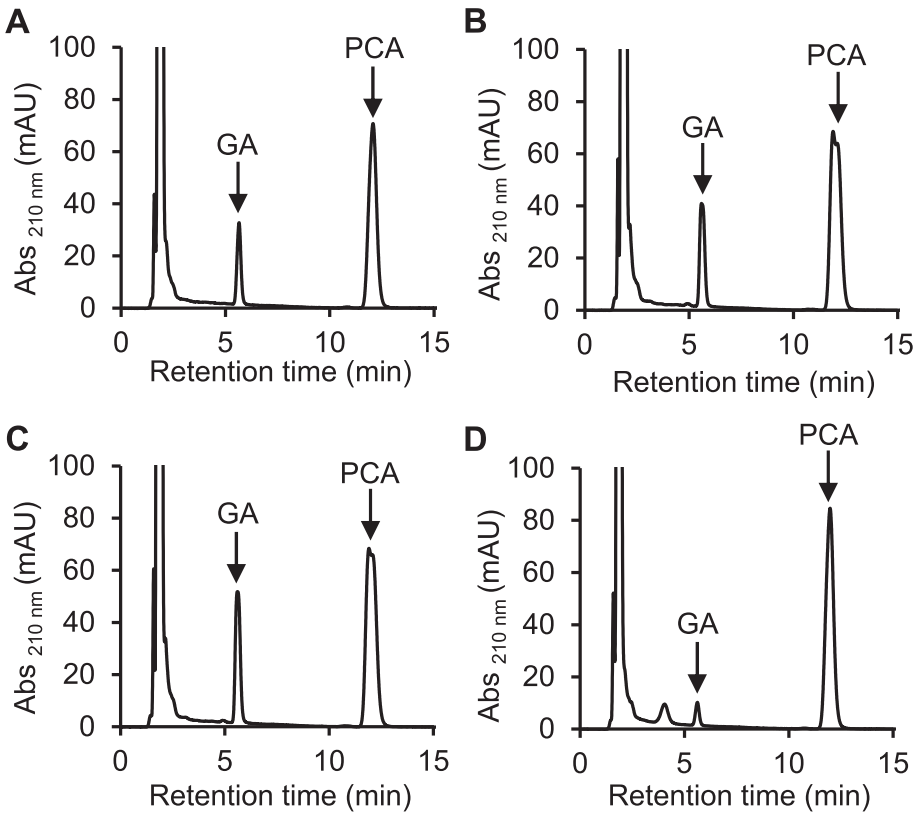

Fig. 3. High-performance liquid chromatography of enzyme products.

Analyses of products generated by 10 μg HgPobA WT (A), HgPobA L207V/Y393F (B), HgPobA T302A/Y393F (C), or PaPobA (D) after reaction at 30°C for 5 min in 20 mM Tris-HCl (pH 7.9) containing 10 μM FAD, 5 mM NADPH, and 1 mM PCA.

Table 3. Steady-state kinetics of reactions between WT and mutant enzymes and substrates.

Enzyme	Substrate	K_m^{app} (μM)	k_{cat}^{app} (s^{-1})	k_{cat}^{app}/K_m^{app} ($\mu M^{-1}\ s^{-1}$)	Coupling ratio (%)
HgPobA WT	*p*HBA	35 ± 14	5.6 ± 0.6	0.16 ± 0.04	83 ± 1
	PCA	260 ± 30	0.74 ± 0.03	0.003 ± 0.001	24 ± 1
L207V/Y393F	*p*HBA	21 ± 14	0.86 ± 0.19	0.041 ± 0.014	66 ± 1
	PCA	90 ± 26	0.76 ± 0.06	0.008 ± 0.002	59 ± 1
T302A/Y393F	*p*HBA	35 ± 8	4.3 ± 0.3	0.12 ± 0.02	78 ± 1
	PCA	76 ± 16	2.3 ± 0.1	0.031 ± 0.005	58 ± 1
PaPobA WT	*p*HBA	24 ± 7	4.7 ± 0.3	0.20 ± 0.04	76 ± 1
	PCA	130 ± 20	0.51 ± 0.02	0.004 ± 0.009	2.2 ± 0.5

Initial velocity of NADPH consumption was measured in 20 mM Tris-HCl (pH 7.9) containing 0.25 mM NADPH, 10 μM FAD, 0–1 mM *p*HBA or PCA, and purified PobA protein at 25°C. Data are shown as means ± standard deviation (n = 3).

generated PCA and GA using HPLC and estimated that the coupling ratios of the reaction (mol PCA and GA/mol NADPH) were 83% and 24% for *p*HBA and PCA, respectively (Table 3). These ratios were comparable between PaPobA for *p*HBA (76%) and quite low (2.2%) for PCA (Table 3), indicating that NADPH oxidation and PCA hydroxylation were more efficiently coupled by HgPobA than PaPobA. This finding was consistent with the increased production of GA by HgPobA, compared with PaPobA (Fig. 3A).

Kinetic properties of HgPobA mutants

The PaPobA L199V/Y385F and the T294A/Y385F mutants hydroxylate PCA faster than wild-type (WT) PaPobA (Chen et al., 2017; Moriwaki et al., 2019). The L199, T294 and Y393 residues of PaPobA respectively corresponded to L207, T302 and Y393 of HgPobA. Therefore, we constructed HgPobA mutants harboring L207V/Y393F and T302A/Y393F mutations. The specific activities for the *p*HBA- and PCA-dependent NADPH oxidation of HgPobA by the L207V/Y393F mutant were 1.4 ± 0.2 and 1.3 ± 0.5 μmol min^{-1} mg^{-1}, respectively. The K_m^{app} and k_{cat}^{app} values of the HgPobA L207V/Y393F mutant reactions were 21 ± 14 μM and 0.86 ± 0.19 s^{-1} for *p*HBA, and 90 ± 26 μM and 0.76 ± 0.060 s^{-1} for PCA, respectively (Table 3). This mutation lowered the k_{cat}^{app} value for *p*HBA 6.5-fold and decreased the K_m^{app} value for PCA by 2.9-fold. The K_m^{app} and k_{cat}^{app} values of the

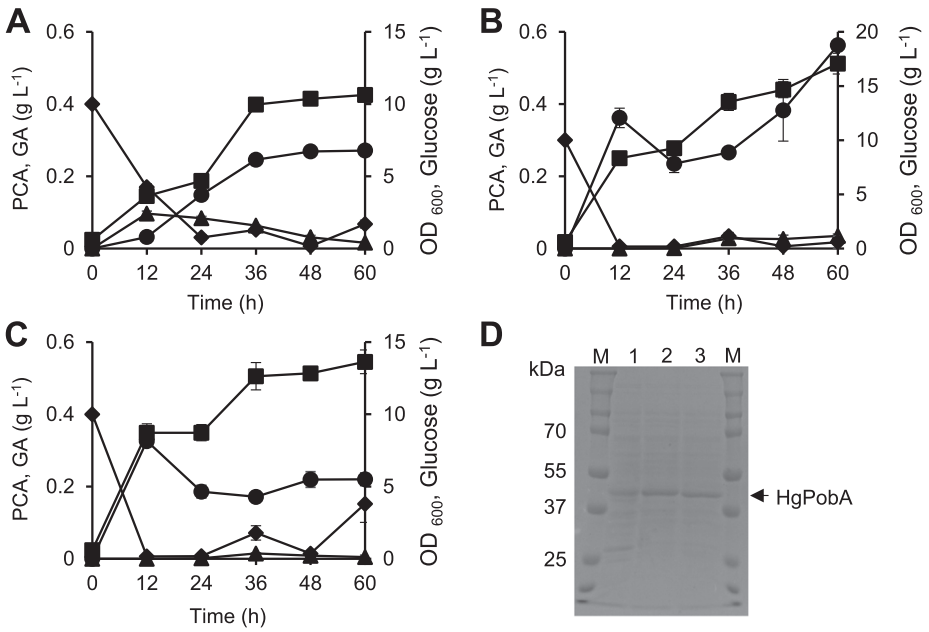

Fig. 4. Fermentation of GA using genetically engineered *E. coli* strains G1 (A), G2 (B), and G3 (C). A–C. Time-course of GA production by *E. coli* strains cultured in fermentation medium (100 mL) containing 1% glucose in 500-mL conical flasks. ●, GA; ▲, PCA; ■, OD_{600}; ◆, Glucose. Data are presented as means ± standard deviation (n = 3). D. SDS-PAGE of HgPobA WT and its mutants in the G1, G2, and G3 strain at 12 h of incubation. M, molecular weight marker; 1, 2, and 3 cell-free extracts (CFEs) of G1, G2, and G3 strains (5 μg each).

reaction by the HgPobA T302A/Y393F mutant were respectively 35 ± 7.7 μM and 4.3 ± 0.28 s^{-1} for *p*HBA (Table 3), whereas these values for PCA were 76 ± 16 μM and 2.3 ± 0.10 s^{-1} and 2.4-fold higher and 6.3-fold lower than those of WT HgPobA. These results indicated that compared with the WT, both HgPobA mutants preferred PCA.

We determined the coupling ratios of the mutant reactions. The comparative coupling ratios of the L207V/Y393F and the T302A/Y393F mutants with *p*HBA compared with WT HgPobA and WT PaPobA were 66%–78% and 76%–83% (Table 3), indicating that *p*HBA is a good substrate for these PobAs. The coupling ratio was 2.4-fold higher (58%) for the reaction between PCA and the mutants than for WT HgPobA and much higher than that between PCA and PaPobA. These results indicated that the mutants increased the preference of HgPobA for PCA.

Fermentation of GA using HgPobA

The finding that HgPobA prefers PCA indicated that it could be useful in an efficient microbial process to produce sugar-based GAs. We therefore constructed an *E. coli* strain that fermented glucose to produce PCA. The *foycjR* gene of the fungus *Fusarium oxysporum* encodes a putative DHS dehydratase that converts the endogenous shikimate pathway intermediate, DHS, to PCA (Fig. 1). The cDNA of this dehydratase was introduced into *E. coli* NST37 (DE3), which has a genetically modified shikimate pathway to maximize DHS production (Masuo et al., 2016) and generate PCA (Fig. 1). Thereafter, HgPobA, HgPobA L207V/Y393F, and HgPobA T302A/Y393F were produced in *E. coli* NST37 (DE3) to obtain the G1, G2, and G3 strains, respectively.

The G1 strain produced 0.27 ± 0.02 and 0.012 ± 0.003 g L^{-1} of GA and PCA, respectively after incubation for 60 h (Fig. 4A). The lower accumulation of PCA indicated that HgPobA hydroxylated PCA to GA. The G2 and the G3 strains accumulated 0.56 ± 0.01 and 0.22 ± 0.02g L^{-1} of GA after the 60-h culture (Fig. 4B, C). The G1, G2, and G3 strains consumed 28, 29, and 26 g L^{-1} of glucose, and respectively yielded 1.0%, 1.9%, and 1.3% GA (*vs.* glucose) during a 60-h incubation. We profiled GA fermentation by the strains during by culture periods. The G2 and G3 strains incubated for 12 h produced 10-fold more GA than the G1 strain incubated for 12 h (0.36 ± 0.01 and 0.33 ± 0.02, respectively, *vs*. 0.032 g L^{-1}; Fig. 4B and C). This finding indicated that the HgPobA mutants increased the PCA hydroxylation rate at the early stages of culture. Intracellular levels of HgPobAs during incubation for 12 h estimated from images of SDS-PAGE gels (Fig. 4D) did not significantly differ. These results coincided with the high activity of the HgPobA mutants towards PCA (Table 2), indicating the mutations of HgPobA positively affected GA fermentation.

After incubation for 12 h, GA accumulation decreased in the G2 and G3 strains over the next 12 h. Glucose availability for producing GA was limited, and a dark brown pigment accumulated, suggesting that some GA oxygen-labile was oxidized (Osawa and Walsh, 1995). During this period, the G1 strain continued to consume glucose and produce GA without accumulating the pigment. These findings are consistent with the notion that culture under glucose-limited conditions accelerates GA degradation. After incubation for 24 h, glucose was added every 24 h to the medium. The G1 and G2 strains gradually accumulated GA during this period, whereas strain G3 did

not, presumably due to missing a factor for GA production. During this incubation period, the G2 and G3 strains consumed 20 and 16 g L^{-1} glucose, respectively (Fig. 4B and C). This implied that strain G3 consumed 1.3-fold less glucose than strain G2, and used less carbon and energy sources for GA production. This could explain the apparent discrepancy in the lower GA production by strain G3 despite producing HgPobA T302A/Y393F, which has a higher k_{cat}/K_m value for PCA than HgPobA L207V/Y393F produced by strain G2 (Table 3).

Discussion

We discovered a novel *p*HBA hydroxylase in *H. gracilis* NS1, HgPobA. This enzyme was active against PCA with K_m ^{app} and k_{cat} ^{app} values for *p*HBA similar to those of PaPobA that typically hydroxylates *p*HBA. These findings indicated that HgPobA functions as a PCA hydroxylase. The ability to hydroxylate PCA is a unique enzymatic feature of known PobAs including PaPobA. A *p*HBA hydroxylase in the *Cupriavidus necator* JMP134 (NCBI accession number, WP_011301134) belongs to the same order (Burkholderiales) as *H. gracilis*, but PCA hydroxylation activity has not been elucidated (Westphal et al., 2018). *Comamonas testosteroni*, like *H. gracilis* belongs to the family Comamonadaceae in the order Burkholderiales and produces a PobA-like 3-hydroxybenzoate 4-hydroxylase that generates PCA (Hiromoto et al., 2006) that does not serve as a reaction substrate. The amino acid similarities of the *Cupriavidus necator* JMP134 and *Comamonas testosteroni* hydroxylases and HgPobA were 64% and 15%, indicating that their structures and functions are diverse among these bacteria.

The crystal structure of PaPobA showed that PCA binds at the active site in a non-productive configuration. That is, the 5-carbon atom of the bound PCA does not face the redox center of the enzyme, which could explain its low k_{cat} for PCA (Schreuder et al., 1988). Our kinetic analyses showed that HgPobA reacts with PCA with a high k_{cat} ^{app} (Table 3), which is in line with the notion that HgPobA binds PCA in a productive configuration that facilitates appropriate hydroxylation (Moriwaki et al., 2019). This is also supported by the higher coupling ratio of NADPH oxidation and PCA hydroxylation by HgPobA than PaPobA (Table 3). These results imply that PCA recognition sites are differently organized between HgPobA and PaPobA, which is consistent with the ability of HgPobA to utilize 2,4-dihydroxybenzoate and *p*-aminobenzoate, neither of which are preferred substrates for PaPobA.

This is the first description of efficient GA fermentation using PobA without artificial amino acid substitution. The recombinant bacteria fermented GA using glucose as a carbon source in a distinctly different process from the bacterial PaPobA that converted either *p*HBA or PCA to very low levels of GA (Chen et al., 2017). The fermentation process developed herein was based on two contradictory reactions: the involvement of and requirement for oxygen in the unfavorable degradation of GA, and for hydroxylating PCA, respectively. This can be overcome by controlling the dissolved oxygen concentration during culture in jar fermenters, which would further enhance GA production using *E. coli* strains.

That HgPobA effectively produced GA through fermentation indicated that GA could be produced by identifying and applying novel natural enzymes that hydroxylate PCA. In fact, the UniProt database contains > 8000 potential microbial PobAs among which, some natural PCA hydroxylases might facilitate GA production and should be the next target of enzymology and fermentation studies.

Acknowledgments

We thank Norma Foster (English Express, North Vancouver, BC, Canada) for critical reading of the manuscript. This study was supported by grants from the Japan Society for the Promotion of Science (JSPS) KAKENHI (JP19H05679 and JP19H05687) to N.T. and the Japan Society for the Promotion of Science (JST SPRING; Grant no: JPMJSP2124) to N.K.

References

Aruoma, OI., Murcia, A., Butler, J., and Halliwell, B. (1983) Evaluation of the antioxidant and prooxidant actions of gallic acid and its derivatives. *J. Agric. Food Chem.*, **41**, 1880–1885.

Badhani, B., Neha, S., and Rita, K. (2015) Gallic acid: A versatile antioxidant with promising therapeutic and industrial applications. *RSC Adv.*, **5**, 27540–27557.

Chen, Z., Chen, T., Shengzhu, Y., and Yi, X. H. (2022) A high-throughput visual screening method for *p*-hydroxybenzoate hydroxylase to increase phenolic compounds biosynthesis. *Biotechnol. Biofuels Bioprod.*, **15**, 1–15.

Chen, Z., Xiaolin, S., Jian, W., Wang, J., Yuan, Q. et al. (2017) Rational engineering of *p*-hydroxybenzoate hydroxylase to enable efficient gallic acid synthesis via a novel artificial biosynthetic pathway. *Biotechnol. Bioeng.*, **114**, 2571–2580.

Diaz-Gomez, R., Lopez-Solis, R., Obreque-Slier, E., and Toledo-Araya, H. (2013) Comparative antibacterial effect of gallic acid and catechin against helicobacter pylori. *Lwt. Food Sci. Technol.*, **54**, 331–335.

Entsch, B., Palfey, B. A., Ballou, D. P., and V. Massey. (1991) Catalytic function of tyrosine residues in *p*-hydroxybenzoate hydroxylase as determined by the study of site-directed mutants. *J. Biol. Chem.*, **266**, 17341–17349.

Eschrich, K., van der Bolt, F. J., de Kok, A., and van Berkel, W. J. (1993) Role of Tyr201 and Tyr385 in substrate activation by *p*-hydroxybenzoate hydroxylase from *Pseudomonas fluorescens*. *Eur. J. Biochem.*, **216**, 137–146

Fujita, T., Nguyen, H. D., Ito, T., Zhou, S., Osada, L. et al. (2013) Microbial monomers custom-synthesized to build true bio-derived aromatic polymers. *Appl. Microbiol. Biotechnol.*, **97**, 8887–8894.

Haslam, E. and Cai, Y. (1994) Plant polyphenols (vegetable tannins): Gallic acid metabolism. *Nat. Prod. Rep.*, **11**, 41–66.

Hiromoto, T., Fujiwara, S., Hosokawa, K., and Yamaguchi, H. (2006) Crystal structure of 3-hydroxybenzoate

hydroxylase from *Comamonas testosteroni* has a large tunnel for substrate and oxygen access to the active site. *J. Mol. Biol.*, **364**, 878–896.

Huo, Y. X., Ren, H., Yu, H., Zhao, L., Yu, S. et al. (2018) CipA-mediating enzyme self-assembly to enhance the biosynthesis of pyrogallol in *Escherichia coli*. *Appl. Microbiol. Biotechnol.*, **102**, 10005–10015.

Hutner, S. H. (1950) Anaerobic and aerobic growth of purple bacteria (Athiorhodaceae) in chemically defined media. *J. Gen. Microbiol.*, **4**, 286–293.

Kambourakis, S., Draths, K. M., and Frost, J. W. (2000) Synthesis of gallic acid and pyrogallol from glucose: Replacing natural product isolation with microbial catalysis. *J. Am. Chem. Soc.*, **122**, 9042–9043.

Kim, T. J., Silva, J. L., and Jung, Y. S. (2011) Enhanced functional properties of tannic acid after thermal hydrolysis. *Food Chem*., **126**, 116–120

Kinugawa, S., Wang, S., Taira, S., Tsuge, A., and Kaneko, D. (2016) Single-molecule interaction force measurements of catechol analog monomers and synthesis of adhesive polymer using the results. *Polym. J.*, **48**, 715–721.

Lara-Victoriano, F., Veana, F., Hernández-Castillo, F. D., Aguilar, C. N., Reyes-Valdés, M. H. et al. (2017) Variability among strains of *Aspergillus* section Nigri with capacity to degrade tannic acid isolated from extreme environments *Arch. Microbiol*., **199**, 77–84.

Luo, Q., Zeng, S., Shu, Y, Fu, Z., Zhao, H. et al. (2018) A novel green process for tannic acid hydrolysis using an internally sulfonated hollow polystyrene sphere as catalyst. *RSC Adv.*, **8**, 17151.

Masuo, S., Zhou, S., Kaneko, T., and Takaya, N. (2016) Bacterial fermentation platform for producing artificial aromatic amines. *Sci. Rep.*, **6**, 1–9.

Maxel, S., Aspacio, D., King, E., Zhang, L., Acosta, A. P. et al. (2020) A growth-based, high-throughput selection platform enables remodeling of 4-hydroxybenzoate hydroxylase active site. *ACS Catal.*, **10**, 6969–6974.

Moriwaki, Y., Yato, Mirai., Terada, T., Saito, S., Nukui N. et al. (2019) Understanding the molecular mechanism underlying the high catalytic activity of *p*-hydroxybenzoate hydroxylase mutants for producing gallic acid. *Biochemistry*, **58**, 4543-4558.

Osawa, R. and Walsh, T. P. (1995) Detection of bacterial gallate decarboxylation by visual color discrimination. *J. Gen. Appl. Microbiol.*, **41**, 165–170.

Rommel, A. and Wrolstad, R. E. (1993) Influence of acid and base hydrolysis on the phenolic composition of red raspberry Juice. *J. Agric. Food Chem.*, **41**, 1237–1241.

Schneider, C. A., Rasband, W. S., and Eliceiri, K. W. (2012) NIH Image to ImageJ: 25 years of image analysis. *Nature Methods*, **9**, 671–675.

Schreuder, H. A., Van der Laan, J. M., Hol, W. G., and Drenth, J. (1988) Crystal structure of *p*-hydroxybenzoate hydroxylase complexed with its reaction product 3,4-dihydroxybenzoate. *J. Mol. Biol.*, **199**, 637–648.

Sileika, T. S., Barrett, D. G., Zhang, R., Lau, K. H. A., and Messersmith, P. B. (2013) Colorless multifunctional coatings inspired by polyphenols found in tea, chocolate, and wine. *Angew. Chem. Int. Ed.*, **125**, 10966–10970.

Spector, T. and Massey, V. (1972) Studies on the effector specificity of *p*-hydroxybenzoate hydroxylase from *Pseudomonas fluorescens*. *J. Biol. Chem.*, **247**, 4679–4687.

Wang, J, Shen, X., Yuan, Q., and Yan, Y. (2018) Microbial synthesis of pyrogallol using genetically engineered *Escherichia coli*. *Metab. Eng.*, **45**, 134–141.

Westphal, A. H., Tischler, D., Heinke, F., Hofmann, S., Gröning, J. A. et al. (2018) Pyridine nucleotide coenzyme specificity of *p*-hydroxybenzoate hydroxylase and related flavoprotein monooxygenases. *Front. Microbiol.*, **9**, 1–17.